µ-XRF Analysis of Trace Elements in Lapis Lazuli-Forming Minerals for a Provenance Study

UNIVERSITÀ DEGLI STUDI DI TORINO

µ-XRF analysis of trace elements in lapis lazuli-forming minerals for a provenance study

µ-XRF potentiality for lapis lazuli provenance

D. Angelici,[ab] A. Borghi,[a] F. Chiarelli,[b] R. Cossio,[a] G. Gariani,[b] A. Lo Giudice,[bc] A. Re,[bc] G. Pratesi[d] and G. Vaggelli[e]

[a] *Dipartimento di Scienze della Terra, Università di Torino, Via Valperga Caluso 35, 10125, Torino, Italy.*

E-mail: debora.angelici@unito.it - Phone: +39(0)11 6707378 - +39(0)11 6707020

[b] *Dipartimento di Fisica, Università di Torino, Via Pietro Giuria 1, 10125, Torino, Italy*

[c] *INFN Sezione di Torino, Via Pietro Giuria 1, 10125, Torino, Italy*

[d] *Museo di Storia Naturale, Università di Firenze, Via G. La Pira 4, 50121 Firenze, Italy*

[e] *CNR - Isitituto di Geoscienze e Georisorse, Via Valperga Caluso 35, 10125, Torino, Italy*

Abstract

This paper presents new developments on the provenance study of lapis lazuli started by our group in 2008: during the years a multi-technique approach has been exploited to obtain a minero-petrographic characterisation and the consequent creation of a database, considering only rock samples of known provenance. Since the final aim of the study is to develop a methodology to analyse archaeological findings and artworks made in lapis lazuli in a completely non-invasive way, Ion Beam Analysis techniques were employed until now to trace back the provenance of the raw material used for the production of artefacts. Continuing on this goal and focusing the analysis on the determination of the more significant minero-chemical markers for the provenance purpose identified as yet (trace elements in different

minerals), the methodology was extended with the use of micro X-ray fluorescence (μ-XRF), testing the potentiality of the technique for this application. The analyses were focused on diopside and pyrite in lapis lazuli samples of known provenance (Afghanistan, Tajikistan and Siberia). In addition, μ-XRF data were compared with μ-PIXE results, verifying the good agreement between the two databases and comparing the analytical performances of both the techniques for this particular application.

Keywords

Lapis lazuli, μ-XRF, μ-PIXE, trace elements, archaeometry, cultural heritage

Introduction

Lapis lazuli is a blue semi-precious stone widely used since the ancient times. The first traces of its use date back to 7000 years ago for different purposes: beads, gems, seals and small decorative artworks were widely distributed in the Ancient East. With the passage of millennia this blue rock continued to be appreciated and used by ancient civilisations, despite its rare occurrence, the limited extension of the quarries and the difficulty to reach them, being located in inaccessible places [Da Cunha, 1989]. The only source of lapis lazuli known in ancient times according to the most widespread opinion were located in Afghanistan [Wyart et al., 1981], although other quarries might have been exploited since antiquity [Herrmann, 1968; Nibbi, 1981; Casanova, 2013] and few of them have been considered in recent studies [Ballirano & Maras, 2006; Zöldföldi et al., 2006]. For this reason a provenance study of lapis lazuli could provide answers to some important issues, for example the use and the dissemination of this rock through the ancient trade routes, answering some open-questions especially for the ancient time when written testimonies are scanty or absent at all [Tosi, 1974].

Lapis lazuli may be either a metamorphic or a magmatic rock whose mineral assemblage is characterised by the widespread or localised occurrence of a blue feldspathoid, mostly lazurite, a sulphur-bearing member of the sodalite group [Hogarth & Griffin, 1976; Hassan et al., 1985]. The paragenesis of lapis lazuli is furthermore composed by a wide variety of mineral phases, the most common are: diopside, wollastonite, calcite, pyrite, k-feldspar, phlogopite [Hogarth & Griffin 1978].

Our study in this field began in 2008 through a multi-technique approach [Lo Giudice et al., 2009] with the aim to obtain petrographic and minero-chemical information in order to identify some peculiar markers reflecting different supplying quarry districts for lapis lazuli. Owing to the complexity and the heterogeneity of the rock and the need of collecting secure results linked to the provenance, the study was started on rock samples of known provenance, coming from four different quarry districts located in Afghanistan (Badakhshan), Tajikistan (Pamir Mountains), Siberia (Lake Baikal area) and Chile (Ovalle).

To speed up the first step of the study, we prepared petrographic sections from the rock samples and their preliminary characterisation by means of optical microscope, cold-cathodoluminescence (cold-CL), μ-Raman Spectroscopy and Scanning Electron Microscopy (SEM-EDX and SEM-CL) permitted to identify the occurrence and distribution of the main mineral phases in the rocks, their chemical composition and their characteristic luminescence spectra. In this way we obtained an appreciable characterisation of these rocks, but since the ultimate goal is the analysis of archaeological findings and artworks made in lapis lazuli using a completely non-invasive approach, we developed a protocol based on extracted-Ion Beam Analyses (IBA) techniques (mainly μ-PIXE: Proton Induced X-ray Emission and μ-IL: IonoLuminescence) [Re et al., 2011; Lo Giudice et al., 2012; Re et al., 2013; Re et al., 2014]. In the last period, to extend the possibilities and to test new accessible facilities, we implemented this protocol employing the micro X-ray fluorescence technique (μ-XRF).

IBA techniques and X-ray fluorescence are widely used for different purposes in the field of Cultural Heritage [Beck, 2014; Calusi, 2011; Mantler & Schreiner, 2000]. First of all because of their potentiality to work in atmosphere and the consequent possibility to analyse precious objects or archaeological findings in a completely non-invasive way without any sampling or surface preparation. Among the other various advantages that permit to both the analytical techniques to be well established in this field, the multi-elemental analysis and the high sensitivity at different elemental range are very important features. A comparative study on glass specimens between IBA- and XRF-based techniques was performed by Sokaras et al. [Sokaras et al., 2009] with the aim to propose an optimized methodology, evaluating advantages and limitations of the different techniques employed, together with the reliability of portable instruments.

In particular, for X-ray fluorescence the more recent μ-XRF instrument development has permitted to overtake many limits of the conventional XRF, allowing to extend its applications not only in art and archaeology but also in many other sectors [Jansse~~s~~ns et al., 2000; Rindby & Janssens, 2002]. The beam size reduction of the order of tens of μm, obtained by mono- or poly-capillary optics to collimate the primary X-ray beam at the sample surface, permits to carry out detailed analysis of an object (its decorations, features or in general all parts forming it to determine the material composition) and reproducible quantitative measurements, preventing systematic errors in quantification due to geometry and sample surface. All the above-mentioned features are fundamental for the aim of this work, i.e. to test the μ-XRF potentialities in the provenance study of lapis lazuli for characterising rock samples and artefacts, as the grain of the lapis lazuli-forming minerals is submillimetric and the minero-chemical markers are mainly to be identified inside the single mineral phases.

In order to find markers useful to trace the provenance of the raw material, we focused our attention on the chemical composition (major and trace elements) of two mineral phases: diopside ($MgCaSi_2O_6$), the mineral phase usually associated to the lazurite in the rocks of Asian provenance and pyrite (FeS_2), one of the main accessory mineral scattered in this blue rock. Furthermore, results obtained on some crystals were compared with μ-PIXE analyses carried out on the same samples and reported in previous works [Re et al., 2011; Lo Giudice et al., 2012; Re et al., 2013; Re et al., 2014].

Materials and Methods

36 samples from lapis lazuli specimens coming from three Asian locations (Afghanistan, Tajikistan and Siberia) were studied (Table 1). They belong to different collections: the Mineralogy and Lithology section of the Museum of Natural History (University of Firenze), the Mineralogical, Petrographical and Geological section of the Regional Museum of Natural Sciences of Torino and the University of Torino. Chilean samples were not taken into account for this work, because they can be well distinguished from the other provenances, by the widespread presence of wollastonite ($CaSiO_3$), absent in all the other samples [Lo Giudice et al., 2009; Calusi et al., 2008; Favaro et al., 2012].

All the analysed samples were prepared as petrographic thin sections (ca. 100 μm thickness) and mounted on plexiglass slides to avoid possible interferences of the glass holder with the excited volume of the sample. The thickness for the petrographic sections was chosen taking into account the attenuation length of X-rays, according to the Henke website (http://henke.lbl.gov/optical_constants/atten2.html), and the penetration depth of the proton beam in the lapis lazuli-forming minerals.

Petrographic examination was undertaken using a polarizing microscope; a scanning electron microscope (SEM; Cambridge Stereoscan S360), equipped with a SDD energy-dispersive spectrometer (EDS; Oxford Instruments), was used for electron microscopy and for

determining the chemical composition of major elements. An accelerating voltage of 15 kV and a dwell time of 60 s were used. Natural silicates and oxides were chosen as standards and a ZAF data reduction program was used. The chemical composition of major elements were also used for the matrix correction routine of μ-XRF quantification.

Micro X-ray fluorescence analyses of trace elements were performed with the μ-XRF Eagle III-XPL, Roentgenanalytik System GmbH & Co. KG, Taunusstein, Germany. It is equipped with a Rh anode (50 kV, 1 mA), polycapillary lens (variable spot size in the range 30 - 300 μm), a set of primary filters (Al [25 μm]; Al [250 μm]; Ti [25 μm]; Ni [25 μm]; Nb [125 μm]; Rh [50 μm]), a ultrapure silicon detector, a stepper motor controlled X-Y-Z stage (100×100×100 mm) and two colour video cameras (visible area of 20×15 mm^2 and 1.5×1.1 mm2, with electronic zoom). The sample chamber (Ø 330×350 mm^3) permits analysis either at atmospheric pressure or in vacuum (ca. 0.5 mbar). Spectral acquisition (using single spot acquisition, profiles or mapping) and quantification are operated by the EDAX Vision 32 software. This instrument has been already employed for a Cultural Heritage applications as the non-destructive study of Islamic glass weights [Vaggelli et al., 2013]. The accuracy for major and minor elements is within 5% and for trace elements around 10%, as reported in [Vaggelli & Cossio, 2012].

In Table 2 the analytical conditions used for diopside and pyrite are listed. Appropriate primary-beam filters were used [Elam et al., 2010] and generally, for each analysed crystal, three measurements at different sample rotation, around the vertical axis, have been carried out in order to eliminate the contribution of diffraction peaks occurring in the crystalline phase.

For the quantification of trace elements the Fundamental Parameters with Standards Method was preferred and used, as extensively discussed in [Vaggelli & Cossio, 2012]. The utilised reference standards are produced by the National Bureau of Standards (NBS); they are the

synthetic glasses SRM 610 and SRM 612, the latter used only for Cu quantification in pyrite. The values corresponding to the "preferred averages" suggested in the work of Pearce et al. [Pearce et al., 1997] were used as certified values for the trace elements quantification.

The limit of detection (LOD) for each trace element of interest were calculated according to the equation reported in [Jenkins et al., 1995] where the nominal concentration for each element of the standard has to be about a factor of ten above the expected detection limits. The equation shows that the LOD value depends on the net peak-to-background ratio, the net peak intensity and the total counting time. The obtained data are reported in Table 3.

Finally, the μ-XRF data were compared with the μ-PIXE results performed on the same samples. μ-PIXE measurements were carried out at the Italian laboratory INFN-LNL AN2000 in-vacuum microbeam facility (2 MeV proton beam) [Bollini et al., 1993] and all the obtained results were gathered and reported in previous works [Re et al., 2011; Re et al., 2013; Re et al., 2014].

Results and Discussion

Diopside

Diopside ($CaMgSi_2O_6$) is a rock-forming silicate mineral belonging to the monoclinic pyroxene series and forming a complete solid solution with hedenbergite ($CaFeSi_2O_6$). It occurs both in many metamorphic and in basic/ultrabasic igneous rocks. The general chemical formula of pyroxene is $M2M1T_2O_6$, where M2 refers to cations in a distorted octahedral coordination, M1 to cations in a regular octahedral coordination and T to tetrahedral coordination. Silicon can be replaced by small amount of Al and other small cations as Fe^{3+} or Ti^{4+}. The Mg (M1) site can also be occupied by Mg-vicariant elements as Fe^{2+}, Al^{3+}, Fe^{3+}, Ti^{3+}, V^{3+}, Cr^{3+}, Zr^{4+} and Mn^{2+}. While Ca (M2) site can be similarly occupied by minor quantities of vicariant elements as Mg^{2+}, Fe^{2+}, Mn^{2+}, Sr^{2+} [Morimoto, 1988]. In addition, diopside ($CaMgSi_2O_6$) can be replaced under metamorphic conditions by jadeite end member

($NaAlSi_2O_6$), a pyroxene variety stable at high P-T conditions in metamorphosed granitoid according to the reaction Albite + Quartz = Jadeite. This substitution is directly proportional to the pressure conditions of recrystallisation [Holland, 1983], in particular Ca and Mg are replaced by Na and Al, respectively, to maintain the balance of the charges according to the following scheme: Na + Al = Ca + Si.

The studied diopside crystals come from lapis lazuli samples of the three provenances considered for this work: Afghanistan, Tajikistan and Siberia. More than 200 crystals were analysed by SEM-EDX system to determine the major elements content. Representative analyses for each provenance are reported in Table 4, while the whole set of data useful for discriminative purposes are represented in Fig. 1. As the graphs show, the data of Afghan and Siberian samples are generally more gathered, differently to the data obtained on samples coming from Tajikistan that are the most scattered. The homogeneity in chemical composition and the low amount of Na and Al characterising the Afghan samples suggest a magmatic origin for this provenance, highlighting that the minimal dispersion of some data are due to only 3 samples of 19 analysed. The wider range of composition for the Tajik samples, with lower Mg and Ca contents and higher Na and Al contents, can be linked to a partial substitution of diopside with the jadeitic end member, suggesting a metamorphic nature for this provenance.

The Siberian samples are characterised by low amount of Na and Al and an average of Ca content (> 19.0 wt.%) which results higher respect to the ideal diopside composition (Ca~18.5). These features can reflect a magmatic nature for the lapis lazuli of this quarry district, associated to a metasomatic process occurred among the surrounding rocks, which are of carbonate composition according to the literature [Aleksandrov & Senin]. Some of these results also contribute to the provenance discrimination: contents of Ca higher than 19.5 wt.%

were observed only in Siberian samples, while contents of Al below 0.7 wt.% were never observed in the samples from Tajikistan.

About trace elements, Tajik samples also show relevant features (Fig. 2): these samples are poor in trace elements (Ti, V, Cr, Mn) unlike the other two provenances, with concentrations of Sr below the LOD in all analysed crystals.

Afghan samples generally present a wider dispersion with higher amount of V (up to 660 ppm) and Cr (up to 740 ppm) and contents of Sr below the LOD. Otherwise, Siberian samples present higher contents of Sr, in the range 400-1200 ppm. In addition, Zr and Pb were detected only in few crystals of the analysed samples and for this reason they are not useful for a provenance discrimination at now.

As regards to minor elements useful for discriminative purposes, Siberian samples present much higher amount of Fe with the median value of about 1230 ppm in the range 500-13000 ppm, compared with the samples from Afghanistan and Tajikistan, respectively about 590 ppm (range 190-4600 ppm) and 350 ppm (range 180-600 ppm).

Comparable results on trace and minor elements were obtained by means of μ-PIXE measurements, for example the comparison on data obtained for V concentrations are shown in Fig. 3, while the whole set of data are entirely discussed in [Re et al., 2014].

Pyrite

Pyrite is a cubic sulphide mineral (FeS_2) that can be found in a wide variety of geological formations being a common accessory mineral in igneous, metamorphic and sedimentary rocks [Bowles et al., 2011]. Among the several studies on trace element contents of minerals, pyrite is the most extensively studied mineral about this topic and a complete review was published by [Abraitis et al., 2004].

About provenance study on lapis lazuli used to make artefacts, pyrite is an ideal mineralogical phase due to the simple chemical formula and because it is easy to quickly find the crystals in an unknown sample or artwork in future studies.

As already highlighted in a previous work focused on pyrite [Re et al., 2013] and confirmed with the present work in conjunction with an increased number of georeferenced samples, all the analysed rocks coming from Siberia are lacking in pyrite crystals. Indeed these samples are characterised by the presence of iron oxide-hydroxide minerals (probable alteration products of pyrite), presenting intensive compositional zoning as showed in Fig. 4. Therefore, the absence of pyrite in lapis lazuli can be used as a macroscopic/microscopic marker to support the Siberian provenance and for this reason it has not been included in the following results. For the other provenances, major elements do not perform any chemical variations useful for discriminative purposes, therefore the analysis was focused on trace elements.

About 100 crystals of pyrite were analysed by means of μ-XRF in the samples coming from Afghanistan and Tajikistan; for these two provenances, trace elements in pyrite (Ni and Cu) came out to be good indicators to discriminate the origin of the samples. The results are shown and compared with μ-PIXE results in Fig. 5.

Pyrite crystals from the Afghan samples present Ni contents above 500 ppm, with a wider dispersion of the experimental points up to 1200 ppm, together with Cu contents below 200 ppm. Pyrite crystals of all samples coming from Tajikistan present low Ni concentrations (below 200 ppm) and Cu contents in the range 200-450 ppm. Consequently, Ni and Cu distributions of the experimental points from Afghan and Tajik quarries plot in well separated fields as shown in Fig. 6. In the graph, the individual errors associated to each measurement carried out by means of both the techniques are represented: the statistical error and the GUPIXWIN output (fit error) [Campbell et al., 2010] were respectively considered for μ-XRF and μ-PIXE measurements.

Comparison between μ-XRF and μ-PIXE results

To evaluate advantages and limitations of the two non-invasive techniques employed in this provenance study of lapis lazuli, μ-XRF analyses on pyrite were compared with μ-PIXE results [Re et al., 2013]. Overall, the graphs of Fig. 5-6 illustrate a good accordance among the distributions of analytical data obtained by means of both the techniques. However, for a more accurate comparison, the single measurements carried out on the same pyrite crystals analysed with the two techniques were selected and compared with each other. Results are shown in Fig. 7, where for Ni only the range below 900 ppm was selected being the more interesting for provenance study and close to the nominal concentration of the standard used, i.e. more reliable for Fundamental Parameters with Standards Method adopted in μ-XRF data analysis. The results obtained by means of the two techniques should be the same and the measured points should lie on a 45° line passing through the origin, represented in the graphs in Fig. 7. This trend is effectively confirmed by the experimental points of Ni and Cu distributions, with tolerable differences probably due to the different probe employed for the analyses and the relative volumes of interaction in the pyrite, as well as the contingent non homogeneity of the analysed crystals. These encouraging results will permit to avoid the use of PIXE technique (and consequently the use of large scale facilities) in the identification of minero-chemical markers useful for the provenance determination, as the case of lapis lazuli here reported.

Conclusion

The database on minero-chemical proprieties of rocks of known origin for the lapis lazuli provenance study was considerably expanded by means of μ-XRF analyses, increasing both the number of samples and measurements and implementing the methodological protocol.

The major elements distribution in diopside can offer indications about the nature of the rock (metamorphic or magmatic) and, together with the information linked to the minor and trace

elements contents, contribute to identify minero-chemical markers for the provenance purpose. Overall, the homogeneity of diopside crystals and the low Na and Al contents in Afghan samples suggest a magmatic nature for this provenance, while the wide variability of chemical composition in the samples from Tajikistan, with a partial substitution of diopside with the jadeitic end member, suggests a metamorphic nature for lapis lazuli quarried from this location. Siberian samples are instead characterised by low amount of Na and Al and high content of Ca, suggesting a magmatic nature followed by a metasomatic alteration process, probably also responsible for the presence of iron oxide-hydroxide minerals (alteration products of pyrite). These samples present also higher amount of Fe, as minor element in diopside.

About trace elements in diopside, the Afghan samples present high content of V and Cr, while high Sr concentrations came out to be a good indicator to discriminate the Siberian provenance. Samples from Tajikistan are characterised by low contents of trace elements, this feature can be connected to a re-immobilisation process during the metamorphism.

Moreover, Afghanistan and Tajikistan provenances can be well distinguished from each other according to the trace element contents in pyrite: Afghan samples are characterised by high amount of Ni, while samples coming from Tajikistan can be identified by relative high contents of Cu and low contents of Ni. Finally, micro X-ray fluorescence is demonstrated to be particularly suitable for the final aim of this study and in general represents a valid and versatile analytical technique in the field of Cultural Heritage studies. The analytical performance (spatial resolution, sensitivity, reproducibility, etc.) fulfils the needs linked to the identification of minero-chemical markers inside the single mineral phases for the provenance determination of lapis lazuli. In addition, the overall agreement with the μ-PIXE database represents a further element about the possibility to use analytical techniques based on bench-top diagnostic tool as μ-XRF, alternately to large scale facilities, for archaeometric purposes.

Acknowledgements

The μ-XRF measures have been obtained with the equipment acquired by the Interdepartmental Center "G. Scansetti" for Studies on Asbestos and Other Toxic Particulates with a grant from Compagnia di San Paolo, Torino, Italy.

Thanks are due to Dr. L. M. Gallo (Regional Museum of Natural Sciences of Torino) for the availability of one Siberian sample.

References

ABRAITIS P.K., PATTRICK R.A.D., VAUGHAN D.J. (2004). Variations in the compositional, textural and electrical properties of natural pyrite: a review. *International Journal of Mineral Processing*, **74**, 41-59.

ALEKSANDROV S. M. & SENIN V.G. (2006). Genesis and Composition of Lazurite in Magnesian Skarns. *Geochemistry International*, **10**, 1053-1067.

BALLIRANO P. & MARAS A. (2006). Mineralogical characterization of the blue pigment of Michelangelo's fresco 'The last judgment'. *American Mineralogist* **91**, 997-1005.

BECK L. (2014). Recent trends in IBA for cultural heritage. *Nuclear Instruments and Methods in Physics Research B* **332**, 439-444.

BOLLINI D., CERVELLARA F., EGENI G.P., MAZZOLDI P., MOSCHINI G., ROSSI P., RUDELLO V. (1993). The microbeam facility of the AN-2000 accelerator of the Laboratori Nazionali di Legnaro. *Nuclear Instruments and Methods in Physics Research A* **328**, 173-176.

BOWLES J.F.W., HOWIE R.A., VAUGHAN J., ZUSSMAN L. (2011). *Rock-forming Mineral. Non-silicates: Oxides, Hydroxides and Sulphides.* Second Edition, Volume 5A. Geological Society of London.

CALUSI S., COLOMBO E., GIUNTINI L., LO GIUDICE A., MANFREDOTTI C., MASSI M., PRATESI G., VITTONE E. (2008). The ionoluminescence apparatus at the LABEC external microbeam facility. *Nuclear Instruments and Methods in Physics Research B* **266**, 2306-2310.

CALUSI S. (2011). The external ion microbeam of the LABEC laboratory in Florence: some applications to Cultural Heritage. *Microscopy and Microanalysis* **17**, 661-666.

CAMPBELL J.L., BOYD N.I., GRASSI N., BONNICK P., MAXWELL J.A. (2010). The Guelph PIXE software package IV. *Nuclear Instruments and Methods in Physics Research B* **268**, 3356-3363.

CASANOVA, M. (2013). *Le lapis-lazuli dans l'Orient Ancien: production et circulation du néolithique au II^{e} millénaire AV.* J.-C. Editions du Comité des travaux historiques et scientifiques, Paris.

DA CUNHA C. (1989). *Le lapis lazuli: son Histoire, ses gisements, se imitations*. Paris, France: Editions du Rocher (in French).

ELAM W.T., SCRUGGS B., NICOLOSI J. (2010). Combined multiple-excitation FP method for micro-XRF analysis of difficult samples. *Powder Diffraction* **25** (2), 182-186.

FAVARO M., GUASTONI A., MARINI F., BIANCHIN S., GAMBIRASI A. (2012). Characterization of lapis lazuli and corresponding purified pigments for a provenance study of ultramarine pigments used in works of art. *Analytical and Bioanalytical Chemistry* **402**, 2195-2208.

GRIEKEN R. V. & MARKOWICA A. (2002). Microbeam XRF - Applications. In *Handbook of X-Ray Spectrometry (Second Edition, Revised and Expanded).* Rindby, A. & Janssens, K., Chapter 11, V. New York: Marcel Dekker.

HASSAN I., PETERSON R.C., GRUNDY H.D. (1985). The structure of lazurite, ideally $Na_6Ca_2(Al_6Si_6O_{24})S_2$, a member of the sodalite group. *Acta Crystallographica* **C41**: 827-832.

HERMANN G. (1968). Lapis Lazuli: the early phases of its trade, Iraq, Vol. **30**, No. 1, 21-57.

HOGART D. D. & GRIFFIN W. (1976). New data on lazurite. *Lithos* **9**, 39-54.

HOGART D. D. & GRIFFIN W. (1978). Lapis lazuli from Baffin Island – a Precambrian meta-evaporite. *Lithos* **11**, 37-60.

HOLLAND T.J.B. (1983). The experimental determination of activities in disordered and short-range ordered jadeitic pyroxenes. *Contributions to Mineralogy and Petrology* **82**, 214-220.

JANSSENS K., VITTIGLIO G., DERAEDT I., AERTS A., VEKEMANS B., VINCZE L., WEI F., DERYCK I., SCHALM O., ADAMS F., RINDBY A., KNÖCHEL A.,

SIMIONOVICI A., SNIGIREV A. (2000). Use of microscopic XRF for non-destructive analysis in art and archaeology. *X-ray Spectrometry* **29**, 73-91.

JENKINS R., GOULD R.W., GEDCKE D. (1995). *Quantitative X-Ray Spectrometry*, 2nd Edition, New York: Marcel Dekker.

LO GIUDICE A., RE A., CALUSI S., GIUNTINI L., MASSI M., OLIVERO P., PRATESI G., ALBONICO M., CONZ E. (2009). Multitechnique characterization of lapis lazuli for provenance study. *Analytical and Bioanalytical Chemistry* **395**, 2211-2217.

LO GIUDICE A., RE A., ANGELICI D., CALUSI S., GELLI N., GIUNTINI L., MASSI M., PRATESI M. (2012). *Analytical and Bioanalytical Chemistry* **404**, 277-281.

MANTLER M. & SCHREINER M. (2000). X-Ray Fluorescence Spectrometry in Art and Archaeology. *X-Ray Spectrometry* **29**, 3-17.

MORIMOTO N. (1988). Nomenclature of pyroxenes. American Mineralogist, Vol. **73**, 1123-1133.

NIBBI A., 1981 - *Ancient Egypt and some Eastern Neighbours,* Park Ridge, Noyes Publication, chap. 2: 33-55.

PEARCE N. J. G., PERKINS W.T., WESTGATE J. A., GORTON M. P., JACKSON S.E., NEAL C.R., CHENERY S. P. (1997). A compilation of New and Published Major and Trace Element Data for NIST SRM 610 and NIST SRM 612 Glass Reference Materials. *The Journal of Geostandards and Geoanalysis* **21**, 115-144.

RE A., LO GIUDICE A., ANGELICI D., CALUSI S., GIUNTINI L., MASSI M., PRATESI G. (2011). Lapis lazuli provenance study by means of micro-PIXE. *Nuclear Instruments and Methods in Physics Research B* **269**, 2373-2377.

RE A., ANGELICI D., LO GIUDICE A., MAUPAS E., GIUNTINI L., CALUSI S., GELLI N., MASSI M., BORGHI A., GALLO L.M., PRATESI G., MANDO' P.A. (2013). New

markers to identify the provenance of lapis lazuli: trace elements in pyrite by means of micro-PIXE. *Applied Physics A* **111**, 69-74.

RE A., ANGELICI D., LO GIUDICE A., CORSI J., ALLEGRETTI S., BIONDI A.F., GARIANI G., CALUSI S., GELLI N., GIUNTINI L., MASSI M., TACCETTI F., LA TORRE L., RIGATO V., PRATESI G. (2014). Ion beam analysis for the provenance attribution of lapis lazuli used in glyptic art: the case of the "Collezione Medicea". Submitted to *Nuclear Instruments and Methods in Physics Research B*.

RINDBY A. & JANSSENS K. (2002). Microbeam XRF. In *Handbook of X-Ray Spectrometry*, Van Grieken R. E. & Markowicz A. A. (ed), chapter 11. New York: Marcel Dekker.

SOKARAS D., KARYDAS A.G., OIKONOMOU A., ZACHARIAS N., BELTSIOS K., KANTARELOU V. (2009). Combined elemental analysis of ancient glass beads by means of ion beam, portable XRF, and EPMA techniques. *Analytical and Bioanalytical Chemistry* **395**, 2199-2209.

TOSI M., (1974). The Lapis Lazuli trade across the Iranian plateau in the 3rd millennium BC. In *Gururājamañjarikā*. Studi in onore di G. Tucci. Istituto Universitario Orientale, pp. 3–22. Napoli, Italy: Istituto Universitario Orientale.

VAGGELLI G. & COSSIO R. (2012). μ-XRF analysis of glasses: a non-destructive utility for cultural heritage applications. *Analyst* **137**, 662-667.

VAGGELLI G., LOVERA V., COSSIO R., MIRTI P. (2013). Islamic glass weights from Egypt. A systematic study by non-destructive μ-XRF technique. *Journal of Non-Crystalline Solids* **363**, 96-102.

WYART J., BARIAND P., FILIPPI J. (1981). Lapis lazuli from Sar-i-Sang, Badakhshan, Afghanistan. *Gems and Gemmology* **17**, 184-190.

ZÖLDFÖLDI J., RICHTER S., KASZTOVSZKY Zs., MIHÁLY J. (2006). Where does lapis lazuli come from? Non-destructive provenance analysis by PGAA. In *Proceeding of the 34th International Symposium on Archaeometry*. Zaragoza - Spain, pp. 353-360.

Tables

Table 1 Number of studied samples according to provenance (AFG: Afghanistan; TAJ: Tajikistan, SIB: Siberia) and collection: MSN_FI (Museum of Natural History, University of Firenze), MRSN_TO (Regional Museum of Natural Sciences of Torino) and UniTO (University of Torino)

	AFG	TAJ	SIB	Catalogue number
MSN_FI	4			RI388, 12397, 47860, AFG_P
		4		RI3063 - RI3066
			12	BK1 - BK7 (SR), BK8 - BK9 (MBR), RI390
MRSN_TO			1	M15920
UniTO	15			AFG_1 - AFG_15

Table 2 µ-XRF analytical conditions for the trace elements acquisition in pyrite and diopside. All the measurements have been performed in vacuum

Analytical conditions	Diopside	Pyrite
Tube voltage (kV)	40	40
Beam current (µA)	1000	500
Process time (µs)	6	10
Primary filter [thickness]	Ni [25µm]	Ti [25µm]
Live time (s)	1000	1000

Table 3 Limit of detection (LOD) calculated for the trace elements of interest, using the nominal concentrations of the reference glass standards, measured in the different analytical conditions used for diopside and pyrite (see Table 2).

Element	**LOD (ppm)**	**LOD (ppm)**
	Diopside	Pyrite
Ti	44	
V	32	
Cr	33	
Mn	26	
Ni		11
Cu		10
Sr	53	

Table 4 Representative SEM-EDX analyses on diopside (expressed in wt.%) for each considered provenance. The measurements below the LOD are indicated by a dash

	AFGHANISTAN			**TAJIKISTAN**			**SIBERIA**		
	AFG5	AFG8	AFG1	RI3063	RI3065	RI3066	BK4-SR	BK10-MBR	BK11-MBR
SiO_7	54.99	55.34	55.58	55.06	55.38	55.69	54.45	54.57	54.04
TiO_2	-	-	1.18	-	-	-	-	-	-
Al_2O_3	1.04	0.32	4.62	5.97	6.29	7.50	0.74	0.20	1.14
FeO	-	-	-	-	-	-	1.19	-	0.17
MgO	17.30	17.76	14.43	14.61	13.99	13.05	15.82	15.82	16.20
CaO	25.71	26.15	20.41	21.79	21.21	19.57	27.30	28.43	27.59
Na_2O	0.53	0.29	3.14	2.69	3.04	3.87	0.47	0.32	0.27
Total	**99.37**	**99.87**	**99.36**	**100.11**	**99.91**	**99.68**	**99.97**	**99.38**	**99.41**

Figure captions

Fig. 1 Major elements composition in diopside (expressed in wt.%) useful for discriminative purpose. Each point is an individual measurement and the box charts represent the dispersion of the experimental points: the median and the two percentile values 0.25 and 0.75. The bars join the minimum and maximum values.

Fig. 2 Trace element contents in diopside (expressed in ppm). Each point is an individual µ-XRF measurement and the box charts represent the dispersion of the experimental points: the median and the two percentile values 0.25 and 0.75. The bars join the minimum and maximum values and the symbols in correspondence to zero value represent the number of measurements below the LOD (as specified at the bottom of each graph).

Fig. 3 Concentration of V in diopside (expressed in ppm). Each point is an individual µ-XRF and µ-PIXE measurement16 and the box charts represent the dispersion of the experimental points: the median and the two percentile values 0.25 and 0.75. The bars join the minimum and maximum values and the symbols in correspondence to zero value represent the number of measurements with V concentrations below the LOD.

Fig. 4 BSE images of a pyrite crystal in a sample from Afghanistan (a) and a representative relict pyrite crystal in a Siberian samples, almost completely altered in iron oxide-hydroxide (b).

Fig. 5 Trace element contents in pyrite (expressed in ppm). Each point is an individual µ-XRF and µ-PIXE measurement15 and the box charts represent the dispersion of the experimental points: the median and the two percentile values 0.25 and 0.75. The bars join the minimum and maximum values and the symbols in correspondence to zero value represent the number of measurements with Ni or Cu concentrations below the LOD.

Fig. 6 Cu vs Ni contents in pyrite from µ-XRF and µ-PIXE measurements. The individual errors associated to each measurement are plotted, while the values below the LOD are represented by a bar indicating the LOD value for each measurement.

Fig. 7 Comparison between µ-XRF and µ-PIXE data (Ni and Cu concentrations) on 18 pyrite crystals analysed by means of both the techniques. For each measurement the relative error is reported and the values below the LOD are represented by a bar indicating the LOD value.

Figure

Fig. 1

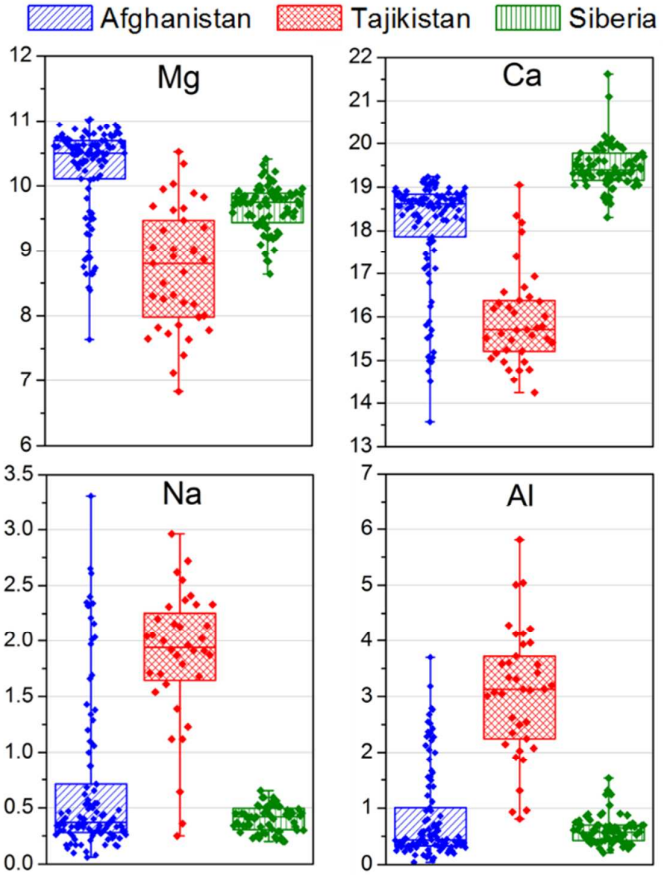

Fig. 2

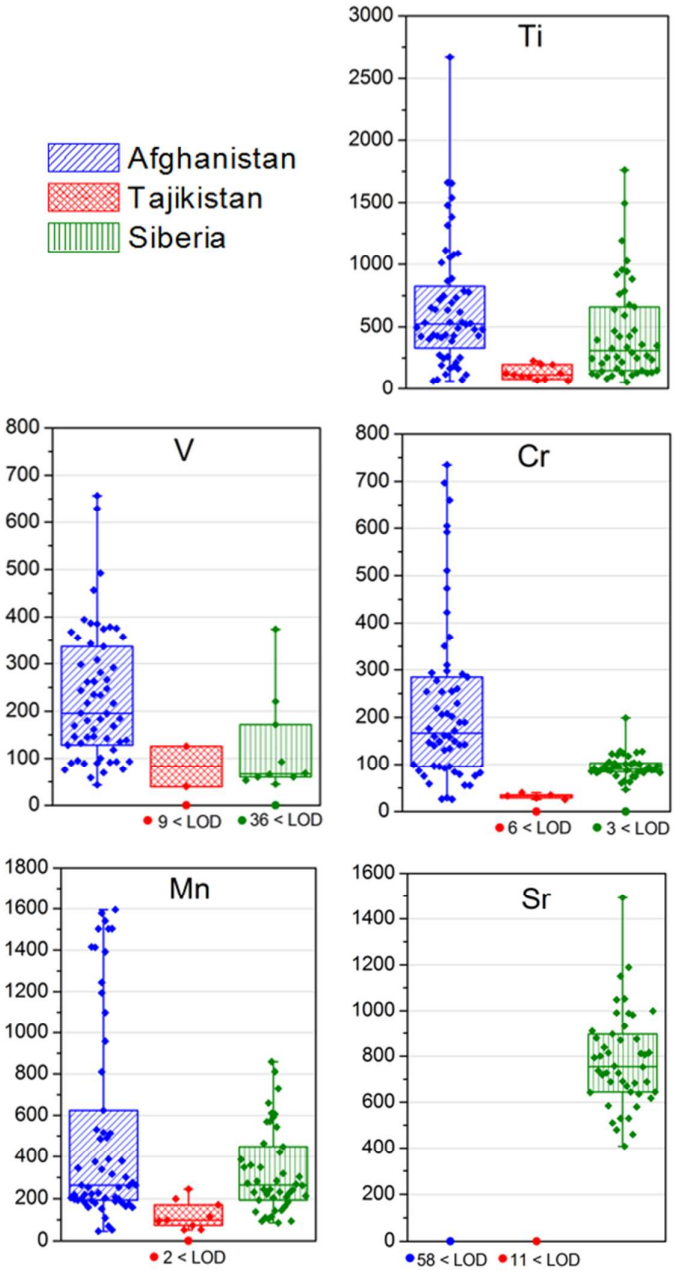
Afghanistan
Tajikistan
Siberia
Ti
V
Cr
Mn
Sr
9 < LOD
36 < LOD
6 < LOD
3 < LOD
2 < LOD
58 < LOD
11 < LOD

Fig. 3

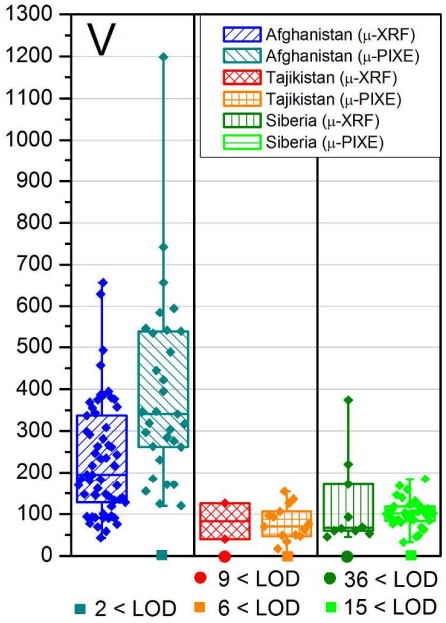

Fig. 4

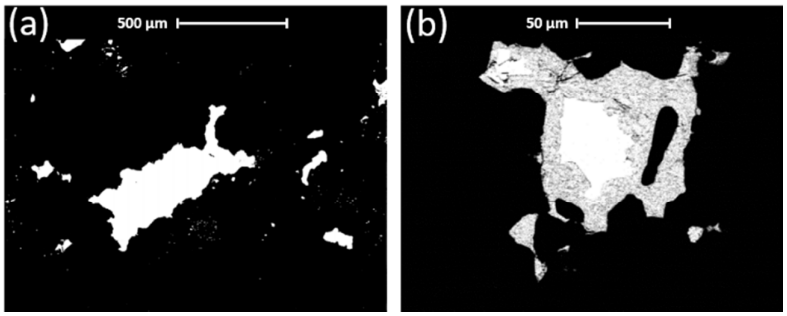

Fig. 5

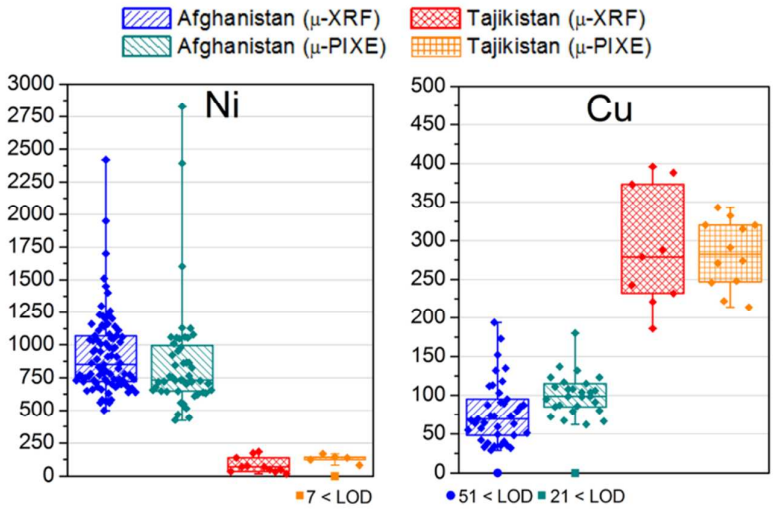

Fig. 6

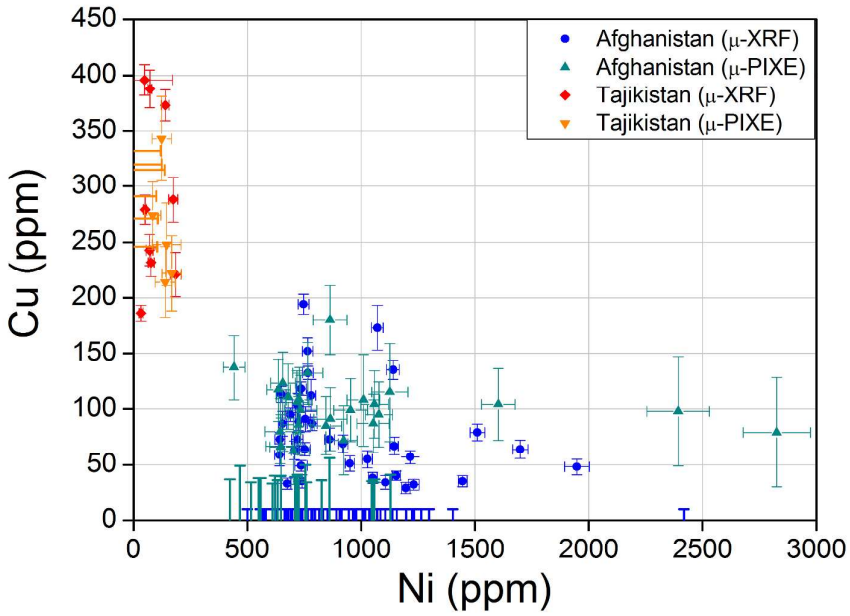
Afghanistan (μ-XRF)
Afghanistan (μ-PIXE)
Tajikistan (μ-XRF)
Tajikistan (μ-PIXE)
Cu (ppm)
Ni (ppm)
0
50
100
150
200
250
300
350
400
450
0
500
1000
1500
2000
2500
3000

Fig. 7

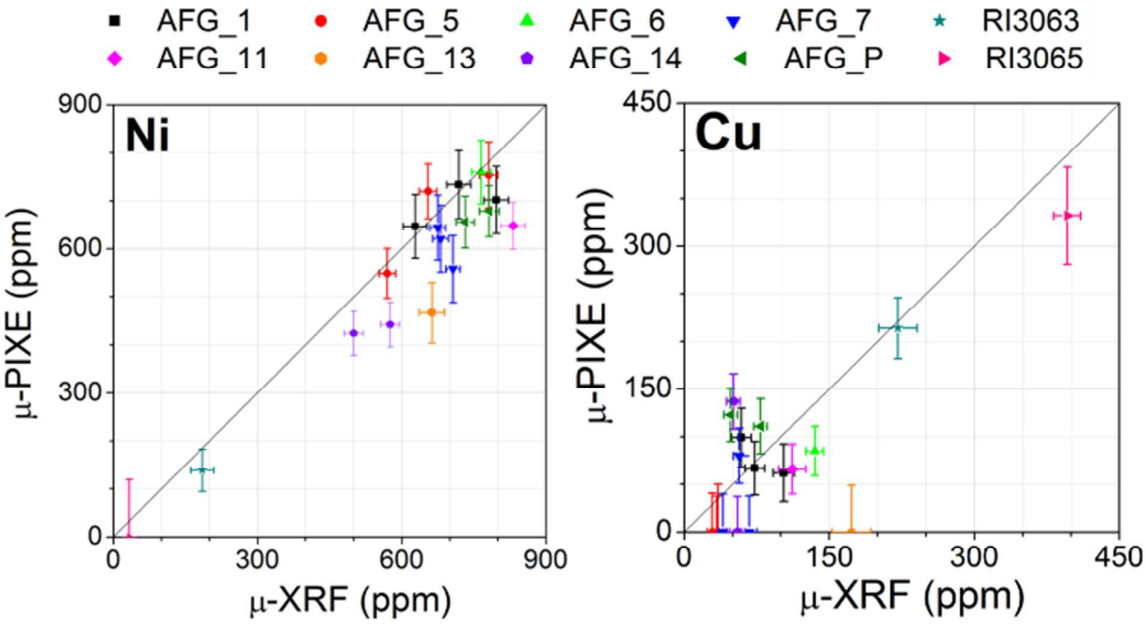
AFG_1
AFG_5
AFG_6
AFG_7
RI3063
AFG_11
AFG_13
AFG_14
AFG_P
RI3065
Ni
μ-PIXE (ppm)
μ-XRF (ppm)
0
300
600
900
Cu
μ-PIXE (ppm)
μ-XRF (ppm)
0
150
300
450